

Unambiguous through-bond sugar-to-base correlations for purines in ^{13}C , ^{15}N -labeled nucleic acids: The $\text{H}_s\text{C}_s\text{N}_b$, $\text{H}_s\text{C}_s(\text{N})_b\text{C}_b$, and $\text{H}_b\text{N}_b\text{C}_b$ experiments

Bennett T. Farmer II^{a,*}, Luciano Müller^a, Edward P. Nikonowicz^b and Arthur Pardi^b

^a*Macromolecular NMR, Pharmaceutical Research Institute, Bristol-Myers Squibb, P.O. Box 4000, Princeton, NJ 08543-4000, U.S.A.*

^b*Department of Chemistry and Biochemistry, University of Colorado at Boulder, Boulder, CO 80309-0215, U.S.A.*

Received 7 September 1993

Accepted 3 November 1993

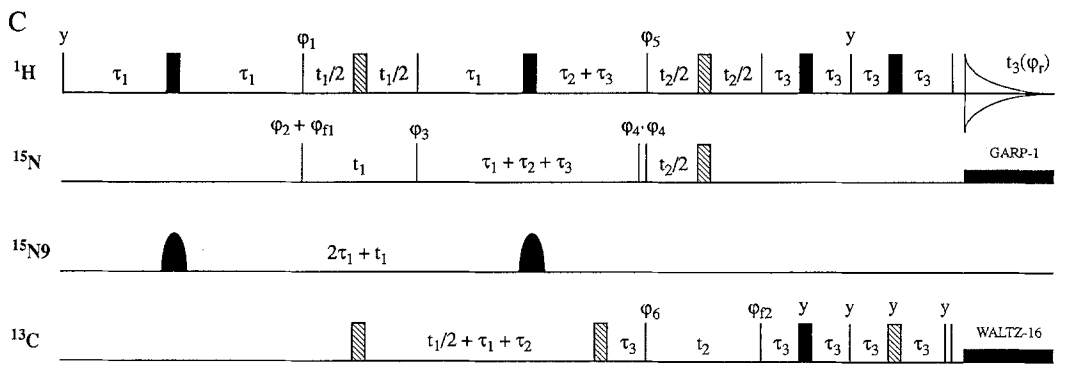
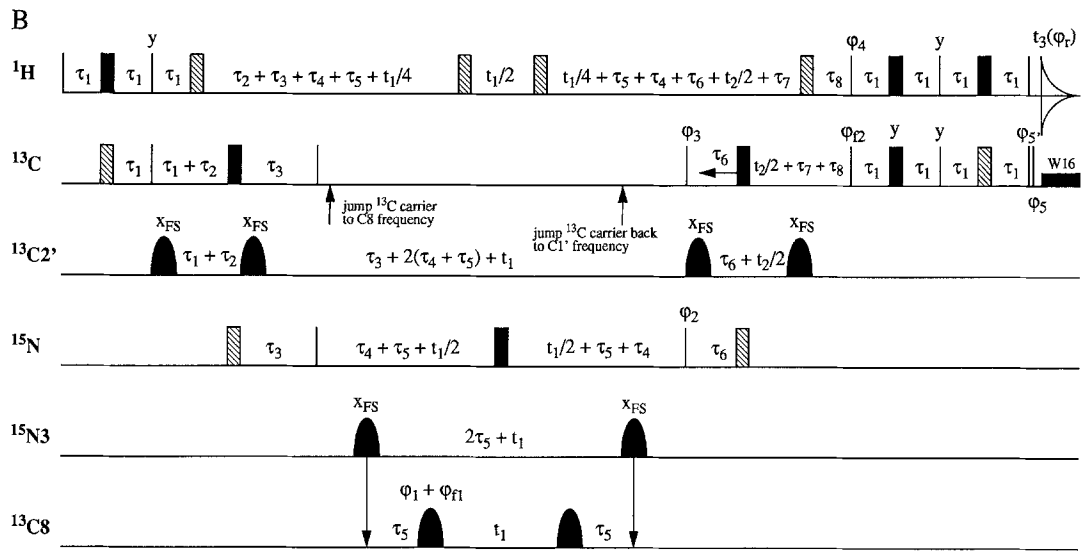
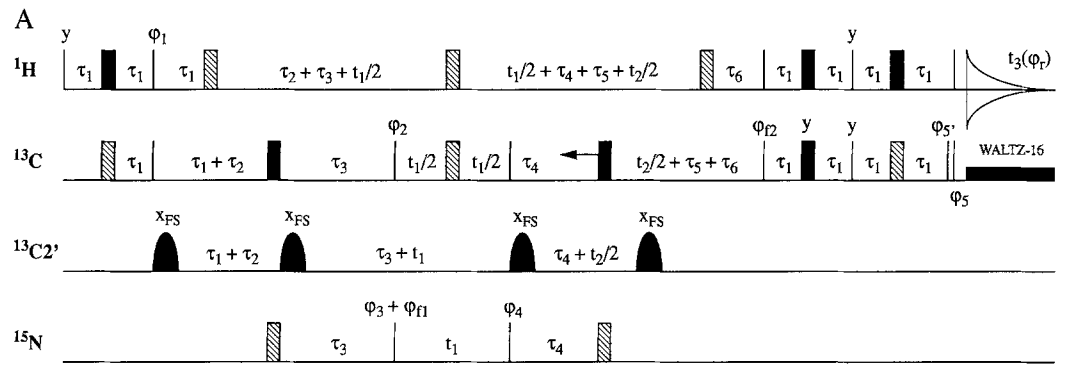
Keywords: Triple-resonance 3D NMR; Isotopically labeled RNA; Purine; Intraresidue sugar-to-base correlations; $\text{H}_s\text{C}_s\text{N}_b$; $\text{H}_s\text{C}_s(\text{N})_b\text{C}_b$; $\text{H}_b\text{N}_b\text{C}_b$

SUMMARY

A set of three 3D (^1H , ^{13}C , ^{15}N) triple-resonance correlation experiments has been designed to provide $\text{H1}'$ - H8 intraresidue sugar-to-base correlations in purines in an unambiguous and efficient manner. Together, the $\text{H}_s\text{C}_s\text{N}_b$, $\text{H}_s\text{C}_s(\text{N})_b\text{C}_b$, and $\text{H}_b\text{N}_b\text{C}_b$ experiments correlate the $\text{H1}'$ sugar proton to the H8 proton of the attached base by means of the $\{\text{H1}', \text{C1}', \text{N9}, \text{C8}, \text{H8}\}$ heteronuclear scalar coupling network. The assignment strategy presented here allows for unambiguous $\text{H1}'$ - H8 intraresidue correlations, provided that no two purines have both the same $\text{H1}'$ and $\text{C1}'$ chemical shifts and the same C8 and N9 chemical shifts. These experiments have yielded $\text{H1}'$ - H8 intraresidue sugar-to-base correlations for all five guanosines in the [^{13}C , ^{15}N] isotopically labeled RNA duplex $r(\text{GGCGCUUGCGUC})_2$.

We have recently reported the first application of a (^1H , ^{13}C , ^{15}N) triple-resonance NMR correlation experiment to [^{13}C , ^{15}N] isotopically labeled RNA (Farmer et al., 1993). This experiment, named $\text{H}_s\text{C}_s(\text{NC})_b\text{H}_b$, in which the *s* and *b* subscripts represent sugar and base resonances, respectively, has unambiguously and efficiently established intraresidue $\text{H1}'$ - H6 correlations for pyrimidines in the 99% ^{13}C , ^{15}N -labeled RNA duplex $r(\text{GGCGCUUGCGUC})_2$ (Farmer et al., 1993; Nikonowicz and Pardi, 1993). The goal of that study was to establish intraresidue sugar proton to base proton correlations, using only through-bond connectivities. For guanosines, however, only G2 yielded an observable $\text{H1}'$ - H8 correlation; furthermore, the intensity of this correlation was 3–5 times weaker than the average intensity of the pyrimidine $\text{H1}'$ - H6 correlations (Farmer et al., 1993). In this communication, we therefore present a complementary set of experiments which provides through-bond intraresidue sugar-to-base correlations in purines.

*To whom correspondence should be addressed.



These triple-resonance experiments have been developed on isotopically labeled mononucleotides, AMP and GMP, and then applied to the isotopically labeled RNA duplex $r(\text{GGCGCUUGCGUC})_2$.

Figure 1 depicts the three 3D (^1H , ^{13}C , ^{15}N) triple-resonance experiments used to unambiguously correlate H1' and C1' of the ribose sugar to N9, C8 and H8 of the base within each purine. The increased complexity of these sequences over their protein-applied counterparts (Ikura et al., 1990; Kay et al., 1990; Olejniczak et al., 1992) is necessitated by the more intricate scalar coupling network within the nucleotide base (vide infra). Using the {H1', C1', N9} heteronuclear scalar coupling network, the $\text{H}_s\text{C}_s\text{N}_b$ experiment in Fig. 1A provides H1'(t₃)-C1'(t₂)-N9(t₁) correlations in purines and affords the most sensitivity. The $\text{H}_s\text{C}_s(\text{N})_b\text{C}_b$ experiment in Fig. 1B is an extension of the $\text{H}_s\text{C}_s\text{N}_b$ experiment and provides H1'(t₃)-C1'(t₂)-(N9)-C8(t₁) correlations in purines by taking advantage of the one-bond N9-C8 heteronuclear scalar coupling ($^1\text{J}_{\text{N9C8}} \sim 9.9$ Hz in GMP, unpublished results). This experiment has, on average, only 10% of the sensitivity of the $\text{H}_s\text{C}_s\text{N}_b$ experiment for guanosine in the isotopically labeled RNA duplex. The delay $\tau_{\text{CN}} = \tau_4 + \tau_5$ in Fig. 1B, during which time N9 coherences evolve to become antiphase to C8, has been optimized at 30 ms for guanosine.

The $\text{H}_b\text{N}_b\text{C}_b$ experiment in Fig. 1C provides H8(t₃)-N9(t₁)-(H8)-C8(t₂) correlations without relying upon the $^1\text{J}_{\text{N9C8}}$ coupling. Instead, the H8-to-N9 coherence transfer step utilizes the $^2\text{J}_{\text{NH}}$ coupling, which is ~ 7.5 Hz for both AMP and GMP (unpublished results). The N9 selective pulses eliminate extraneous H8-N7 correlations in purines, minimize H6-N1 correlations in pyrimidines, and help increase the sensitivity of the $\text{H}_b\text{N}_b\text{C}_b$ experiment. The transfer pathway for the $\text{H}_b\text{N}_b\text{C}_b$ experiment was chosen so that direct transfer of magnetization from C8 to N9 was not necessary. Such a direct transfer is difficult to achieve efficiently, due to the complex homonuclear coupling network for C8 ($^2\text{J}_{\text{C8C4}} \sim 8.6$ Hz and $^2\text{J}_{\text{C8C5}} \sim 6.7$ Hz in GMP, unpublished results), the spectral proximity of C4 to C8, and the intrinsic dispersion of the C8 resonances.

The 3D $\text{H}_s\text{C}_s\text{N}_b$, $\text{H}_s\text{C}_s(\text{N})_b\text{C}_b$, and $\text{H}_b\text{N}_b\text{C}_b$ experiments in Fig. 1 have been applied to the 99% ^{13}C , ^{15}N -labeled RNA duplex $r(\text{GGCGCUUGCGUC})_2$ (Nikonowicz and Pardi, 1993). Figure 2

←

Fig. 1. The $\text{H}_s\text{C}_s\text{N}_b$, $\text{H}_s\text{C}_s(\text{N})_b\text{C}_b$, and $\text{H}_b\text{N}_b\text{C}_b$ 3D (^1H , ^{13}C , ^{15}N) triple-resonance sequences used to establish intrasidic sugar-to-base correlations in ^{13}C , ^{15}N -labeled RNA. 90° pulses are represented by narrow lines, simple 180° pulses by black rectangles, and composite $90_x240_x90_x$ inversion pulses (Levitt, 1986) by diagonally striped rectangles. Pulses on lines labeled with a particular *spin group* (not just the nucleus) are Gaussian-shaped pulses (64 steps, 5σ cutoff) selective for that spin group. Complex data were collected in t₁ by the hypercomplex-TPPI method (Marion et al., 1989) with FIDs for $\varphi_{t1} = x, y$ being stored separately. Complex data were collected in t₂ with FIDs for $\varphi_{t2} = (x, -x)$ (Palmer II et al., 1991) being stored separately. Each 3D hypercomplex data set was processed as previously described (Palmer II et al., 1991) to achieve a quadrature-detected, phase-sensitive display along the F₁ and C1' dimensions, with sensitivity enhancement for the C1' dimension. (A) $\text{H}_s\text{C}_s\text{N}_b$ sequence. The subscript FS, appended to certain pulse phases, denotes a frequency-shifted pulse, achieved by a linear phase ramp (Patt, 1992). The horizontal arrow in front of the ^{13}C 180° refocussing pulse during the constant-time t₂ period indicates that this pulse is moved progressively to the left as t₂ increases. The phase cycle is: $\varphi_1 = 4(x), 4(-x)$; $\varphi_2 = 2(x), 2(-x)$; $\varphi_3 = x, -x$; $\varphi_4 = 16(x), 16(-x)$; $\varphi_5 = 8(x), 8(-x)$; $\varphi_6 = \varphi_5 + \pi/2$; and $\varphi_r = \varphi_1 + \varphi_2 + \varphi_3 + \varphi_4$. (B) $\text{H}_s\text{C}_s(\text{N})_b\text{C}_b$ sequence. The frequency jump to position the ^{13}C carrier in the middle of the C8 spin group is accomplished with a phase-continuous synthesizer, so that a reproducible phase relationship between all pulses on ^{13}C nuclei is maintained. The t₂ evolution is conducted in a constant-time manner. The phase cycle is: $\varphi_1 = x, -x$; $\varphi_2 = 2(x), 2(-x)$; $\varphi_3 = 4(x), 4(-x)$; $\varphi_4 = 8(x), 8(-x)$; $\varphi_5 = 16(x), 16(-x)$; $\varphi_6 = \varphi_5 + \pi/2$; and $\varphi_r = \varphi_1 + \varphi_2 + \varphi_3 + \varphi_4$. (C) $\text{H}_b\text{N}_b\text{C}_b$ sequence. The phase cycle is: $\varphi_1 = 4(x), 4(-x)$; $\varphi_2 = x, -x$; $\varphi_3 = 32(x), 32(-x)$; $\varphi_4 = 16(x), 16(-x)$; $\varphi_5 = \varphi_4 + \pi/2$; $\varphi_6 = 8(x), 8(-x)$; $\varphi_7 = 2(x), 2(-x)$; and $\varphi_r = \varphi_1 + \varphi_2 + \varphi_3 + \varphi_5 + \varphi_6$.

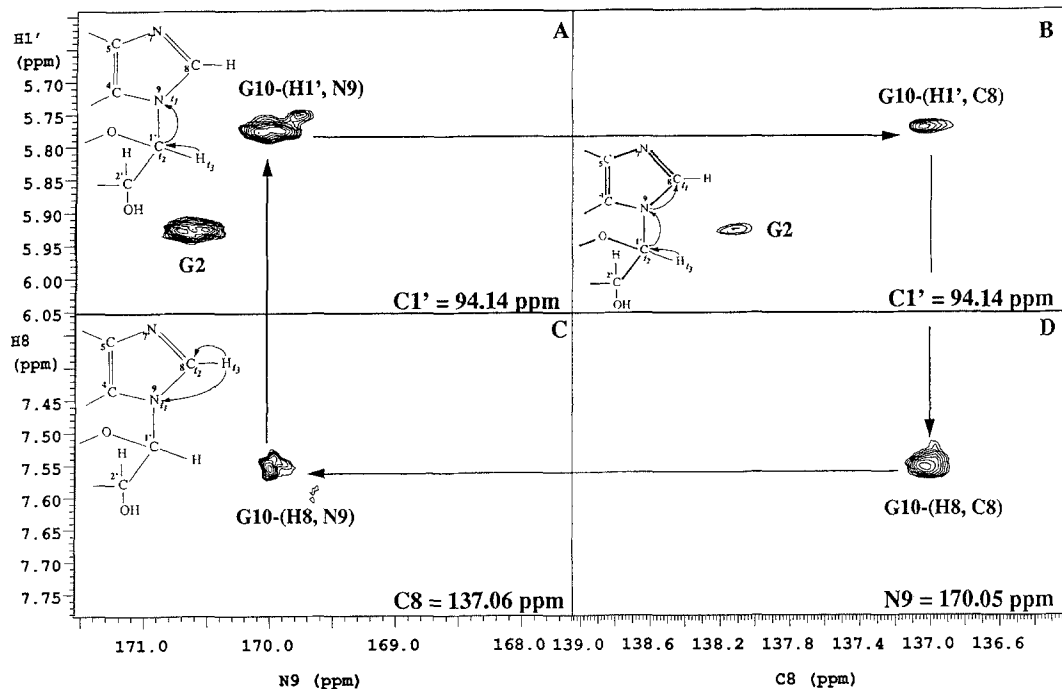


Fig. 2. 2D planes of the 3D triple-resonance experiments used to establish the intraresidue sugar-to-base correlation for G10 in the ^{13}C , ^{15}N -labeled RNA duplex. All spectra were recorded at 30 °C on a standard, three-channel UNITY 600 spectrometer. The insets in Figs. 2A–C, which depict the relevant purine structure, illustrate the magnetization transfer pathway that is employed in the $\text{H}_s\text{C}_s\text{N}_b$, $\text{H}_s\text{C}_s(\text{N})_b\text{C}_b$, and $\text{H}_b\text{N}_b\text{C}_b$ experiments, respectively. (A) The $\text{H}_s\text{C}_s\text{N}_b$ $\text{H1}'\text{-N9}$ 2D plane at the G10 $\text{C1}'$ chemical shift. (B) The $\text{H}_s\text{C}_s(\text{N})_b\text{C}_b$ $\text{H1}'\text{-C8}$ 2D plane at the G10 $\text{C1}'$ chemical shift. No N3 selective inversion pulses were applied here, because there are no adenosines in this RNA fragment. (C) The $\text{H}_b\text{N}_b\text{C}_b$ $\text{H8}\text{-N9}$ 2D plane at the G10 C8 chemical shift. (D) The $\text{H}_b\text{N}_b\text{C}_b$ $\text{H8}\text{-C8}$ 2D plane at the G10 N9 chemical shift. Acquisition parameters common to all three experiments: $t_{90}(\text{H}) = 7.5 \mu\text{s}$, $t_{90}(\text{C}) = 13.4 \mu\text{s}$, $t_{90}(\text{N}) = 37 \mu\text{s}$, and $\text{sw}(\text{H}) = 3 \text{ kHz}$, $t_3(\text{H1}') = 120.0 \text{ ms}$. Additional $\text{H}_s\text{C}_s\text{N}_b$ (Fig. 2A) acquisition parameters: $t_{180}(\text{C2}') = 896 \mu\text{s}$, frequency-shifted by -2550 Hz (Patt, 1992), $\gamma\text{B}_2(\text{C1}' \text{ decouple}) = 1.29 \text{ kHz}$, using WALTZ-16 (Shaka et al., 1983), $\text{sw}(\text{C1}') = 600.0 \text{ Hz}$, $t_2^{\text{max}}(\text{C1}') = 33.33 \text{ ms}$, $\text{sw}(\text{N9}) = 800.0 \text{ Hz}$, $t_1^{\text{max}}(\text{N9}) = 38.75 \text{ ms}$, $\tau_1 = 1.48 \text{ ms}$, $\tau_2 = 18.52 \text{ ms}$, $\tau_3 = 20.00 \text{ ms}$, $\tau_4 = \tau_3 - (t_2/2)$, $\tau_5 = \tau_2 - (\tau_2/2)$, and $\tau_6 = \tau_1 + (t_2/2)$. Additional $\text{H}_s\text{C}_s(\text{N})_b\text{C}_b$ (Fig. 2B) acquisition parameters: $t_{180}(\text{C2}') = 896 \mu\text{s}$, frequency-shifted by -2550 Hz , $t_{90}(\text{C8}) = 704 \mu\text{s}$, $\gamma\text{B}_2(\text{C1}' \text{ decouple}) = 1.29 \text{ kHz}$, using WALTZ-16, $\text{sw}(\text{C1}') = 600.0 \text{ Hz}$, $t_2^{\text{max}}(\text{C1}') = 33.33 \text{ ms}$, $\text{sw}(\text{C8}) = 650.0 \text{ Hz}$, $t_1^{\text{max}}(\text{C8}) = 35.38 \text{ ms}$, $\tau_1 = 1.48 \text{ ms}$, $\tau_2 = 18.52 \text{ ms}$, $\tau_3 = 20.00 \text{ ms}$, $\tau_A = 15.00 \text{ ms}$, $\tau_4 = \tau_A - (t_1/4)$, $\tau_5 = \tau_A + (t_1/4)$, $\tau_6 = \tau_3 - (t_2/2)$, $\tau_7 = \tau_2 - (t_2/2)$, and $\tau_8 = \tau_1 + (t_2/2)$. In the $\text{H}_b\text{N}_b\text{C}_b$ experiment, the ^{13}C carrier frequency for C8 was 7050.0 Hz downfield with respect to that for $\text{C1}'$. Additional $\text{H}_b\text{N}_b\text{C}_b$ (Figs. 2C and D) acquisition parameters: $t_{180}(\text{N9}) = 750 \mu\text{s}$, $\gamma\text{B}_2(\text{C8} \text{ decouple}) = 0.81 \text{ kHz}$, using WALTZ-16, $\gamma\text{B}_3(\text{N7/9} \text{ decouple}) = 1.21 \text{ kHz}$, using GARP-1 (Shaka et al., 1985) at a carrier frequency 2.13 kHz downfield of the N9 resonances, $\text{sw}(\text{C8}) = 905.2 \text{ Hz}$, $t_2^{\text{max}}(\text{C8}) = 25.41 \text{ ms}$, $\text{sw}(\text{N9}) = 240.0 \text{ Hz}$, $t_1^{\text{max}}(\text{N9}) = 62.5 \text{ ms}$, $\tau_1 = 13.00 \text{ ms}$, $\tau_2 = 11.84 \text{ ms}$, and $\tau_3 = 1.16 \text{ ms}$. The total acquisition times were: 43 h ($\text{H}_s\text{C}_s\text{N}_b$); 37 h ($\text{H}_s\text{C}_s(\text{N})_b\text{C}_b$); and 43 h ($\text{H}_b\text{N}_b\text{C}_b$). The final 3D $\text{F}_1\text{F}_2\text{F}_3$ spectral data sizes in real points were: $256 \times 128 \times 1024$ ($\text{H}_s\text{C}_s\text{N}_b$); $128 \times 128 \times 1024$ ($\text{H}_s\text{C}_s(\text{N})_b\text{C}_b$); and $128 \times 128 \times 1024$ ($\text{H}_b\text{N}_b\text{C}_b$).

illustrates the strategy for establishing intraresidue sugar-to-base correlations in guanosine. Figures 2A and B display the 2D ($\text{H1}'$, N9) plane from the $\text{H}_s\text{C}_s\text{N}_b$ experiment and the 2D ($\text{H1}'$, C8) plane from the $\text{H}_s\text{C}_s(\text{N})_b\text{C}_b$ experiment, respectively, at the $\text{C1}'$ chemical shift for G10 (94.14 ppm) (Nikonowicz and Pardi, 1993). Due to overlap between G10 and G2 in the $\text{C1}'$ dimension, these planes also show both the G2 $\text{H1}'\text{-N9}$ and $\text{H1}'\text{-C8}$ correlation peaks, respectively, which are

resolved from G10 by differences in the H1', N9 and C8 chemical shifts. Figures 2C and D display the 2D (H8,N9) and the 2D (H8,C8) planes, respectively, from the $H_bN_bC_b$ experiment. The horizontal lines between Figs. 2A and B at the G10 H1' chemical shift and between Figs. 2C and D at the G10 H8 chemical shift independently identify the N9 and C8 resonances for this nucleotide. The vertical lines between Figs. 2A and C and between Figs. 2B and D link the two independent sets of correlations together, establishing the H1'-H8 correlation for G10 through both the N9 (Figs. 2A and C) and C8 (Figs. 2B and D) chemical shifts. With these data, the G10 H1' and C1' sugar resonances are readily correlated with the base H8, C8 and N9 resonances. The strategy presented here allows for unambiguous intraresidue sugar-to-base correlations, provided that no two purines have both the same H1' and C1' chemical shifts and the same C8 and N9 chemical shifts.

The set of triple-resonance experiments presented in Fig. 1 has yielded H1'-H8 intraresidue sugar-to-base correlations for all five guanosines in this isotopically labeled RNA duplex. Although the duplex contains no adenosines, experiments on isotopically labeled AMP and GMP indicate that the $H_sC_sN_b$ experiment is equally sensitive for adenosine and guanosine, that the $H_bN_bC_b$ experiment is 50% more sensitive for adenosine, and that the $H_sC_s(N)_bC_b$ experiment is a factor of 2.2 more sensitive for adenosine than for guanosine, but only if one individually optimizes τ_{CN} for each nucleotide (unpublished results). We therefore expect that these triple-resonance experiments should work at least as well for adenosine as they do for guanosine in isotopically labeled oligonucleotides. Further studies are under way to establish the efficacy of these experiments, as well as of the $H_sC_s(NC)_bH_b$ experiment (Farmer et al., 1993), on larger isotopically labeled RNAs.

ACKNOWLEDGEMENTS

This work was supported by NIH grant AI33098 and NIH Research Career Development Award AI01051 to A.P. and by an NIH NRSA Fellowship to E.P.N. We also thank the W.M. Keck Foundation for its generous support of RNA science on the Boulder campus.

REFERENCES

- Farmer II., B.T., Müller, L., Nikonowicz, E.P. and Pardi, A. (1993) *J. Am. Chem. Soc.*, **115**, 11040–11041.
 Ikura, M., Kay, L.E. and Bax, A. (1990) *Biochemistry*, **29**, 2659–2667.
 Kay, L.E., Ikura, M., Tschudin, R. and Bax, A. (1990) *J. Magn. Reson.*, **89**, 496–514.
 Levitt, M.H. (1986) *Prog. NMR Spectrosc.*, **18**, 61–122.
 Marion, D., Ikura, M., Tschudin, R. and Bax, A. (1989) *J. Magn. Reson.*, **85**, 393–399.
 Nikonowicz, E.P. and Pardi, A. (1993) *J. Mol. Biol.*, **232**, 1141–1156.
 Olejniczak, E.T., Xu, R.X., Petros, A.M. and Fesik, S.W. (1992) *J. Magn. Reson.*, **100**, 444–450.
 Palmer II, A.G., Cavanagh, J., Wright, P.E. and Rance, M. (1991) *J. Magn. Reson.*, **93**, 151–170.
 Patt, S.L. (1992) *J. Magn. Reson.*, **96**, 94–102.
 Shaka, A.J., Keeler, J., Frenkiel, T. and Freeman, R. (1983) *J. Magn. Reson.*, **52**, 335–338.
 Shaka, A.J., Barker, P. and Freeman, R. (1985) *J. Magn. Reson.*, **64**, 547–552.